Bogdan SAPIŃSKI*

MAGNETORHEOLOGICAL DAMPERS IN VIBRATION CONTROL OF MECHANICAL STRUCTURES

SUMMARY

The paper summarizes the experimental data gathered during the laboratory tests of vibration control of three mechanical structures utilizing magnetorheological (MR) dampers. The author's research program involved the investigations of the structures. The first application refers to vibration control in a driver's seat suspension (structure 1). The control objective is to reduce vertical acceleration of the driver. The second application covers vibration control in a pitch plane vehicle suspension (structure 2). The control objective is to reduce vertical and angular accelerations of the vehicle. The third application concerns vibration control of a suspended cable (structure 3). The control objective is to reduce transverse free vibrations of the cable. The obtained results demonstrate system performance improvement achieved through the control of MR damper(s).

Keywords*: MR damper, vibration control, mechanical structure*

TŁUMIKI MAGNETOREOLOGICZNE W STEROWANIU DRGANIAMI STRUKTUR MECHANICZNYCH

W artykule podsumowano wyniki badań laboratoryjnych prowadzonych pod kierunkiem autora nad sterowaniem drganiami trzech struktur mechanicznych z zastosowaniem tłumików magnetoreologicznych (MR). Pierwsza aplikacja dotyczyła sterowania drganiami zawieszeniu fotela kierowcy (struktura 1). Celem sterowania była redukcja przyspieszenia drgań kierowcy. Druga aplikacja dotyczyła sterowania drganiami zawieszenia pojazdu (struktura 2). Celem sterowania była redukcja przyspieszenia drgań pionowych i kątowych pojazdu. Trzecia z aplikacji dotyczyła sterowania drganiami zawieszonej liny (struktura 3). Celem sterowania była redukcja drgań swobodnych liny. Wyniki eksperymentów wykazały skuteczność tłumików MR do sterowania drganiami badanych struktur.

Słowa kluczowe*: tłumiki MR, sterowanie drganiami, struktury mechaniczne*

1. INTRODUCTION

MR dampers, used commercially since the mid-1990s, are of major interest for researchers and practitioners. The efficacy of MR dampers for providing real-time control has lead to spectacular engineering applications in the past decade.

MR dampers are energy-dissipating devices controlled by a magnetic field. They contain MR fluid which has the capability of reversibly changing from free-flowing, viscous liquids to semi-solids having a controllable yield strength within milliseconds, when exposed to the magnetic field. The functional relationship between damping force and velocity in MR dampers is adjustable by the magnetic field control that changes viscosity of MR fluid filling the dam-pers. The actuation process in MR dampers allows us to modify the damping characteristics under varying conditions.

The paper summarizes results of experiments conducted to control vibrations in three mechanical structures: a driver's seat suspension, a vehicle suspension and a suspended cable. To control vibrations we utilize commercially available MR dampers. The control objective is to reduce vibrations of the structures.

2. MR DAMPERS

The schematic diagram of an MR damper is illustrated in Figure 1. In this arrangement ports 1 and 2 represent mechanical power as the product of velocity and force, while the port 3 represents the control input through the applied magnetic field.

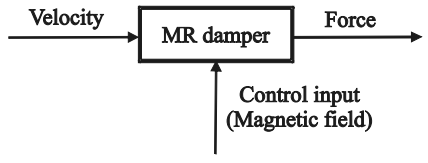

Fig. 1. Schematic diagram of an MR damper

A simplified force-velocity relationship for an MR damper (Fig. 2) shows that a minimum damping ratio occurs in the absence of magnetic fields (zero current). Under magnetic field control and maximum current, the damper is capable of developing a maximum force across the entire velocity range. The boundaries of zero current, maximum current, and maximum positive and negative velocity define a symmetrical envelope for the force-velocity map required of the MR damper, within and across which it will operate under control, as demanded.

* Department of Process Control, AGH University of Science and Technology Krakow, Poland

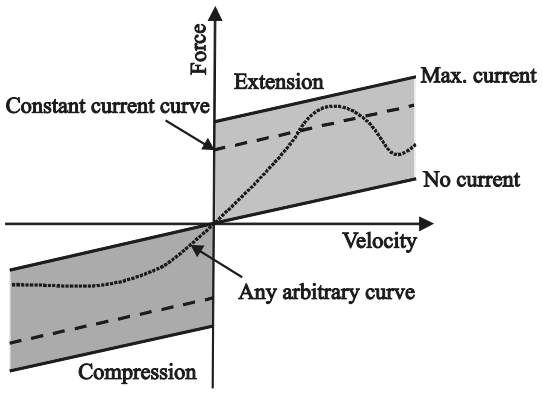

Fig. 2. Force vs. velocity for an MR damper

In the investigated structures we used MR dampers of Lord Co. In structures 1 and 2 we employed the RD-1005-3 dampers, and in structure 3 the RD-1097-1 damper (http://www.lord.com).

The structure of the RD-1005-3 which is recommended for suspended seat applications in heavy trucks and off-highway vehicles is shown in Figure 3. The piston and ring create the control valve for the fluid flow. The flow is controlled by a magnetic field induced in the valve. The magnetic field is generated by the current in the coil which is incorporated in the piston.

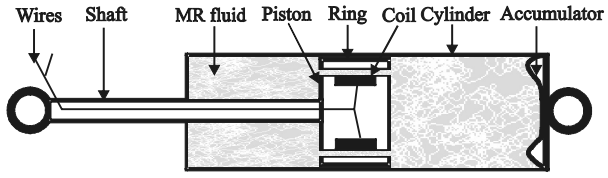

Fig. 3. Structure of the RD-1005-3 damper

The structure of the RD-1097-1 which is damper recommended for experimental use only is provided in Figure 4.

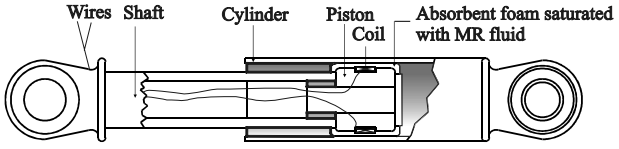

Fig. 4. Structure of the RD-1097-1 damper

The main benefits of RD-100-3 and RD-1097-1 dampers are: low voltage and current requirements, simple electronics and real time control.

3. GENERAL CHARACTERIZATION OF THE INVESTIGATED SYSTEMS

Vibration control systems utilizing MR dampers belong to the category of semi-active systems. The origins of semi-active systems go back to research work where potentials were explored for improving the properties of vibration reduction systems through modulation of parameters of nominally passive components, such as springs or dampers. In such systems, actuators control the parameters of passive components (stiffness and damping), adjusting their value to the operating conditions, in accordance with the predetermined performance index. Capable of fast changes in parameter values, semi-active systems have major advantages, as they reduce the amplitude gain of vibrations transmitted on the vibrating system in the resonance frequency range without deteriorating vibration isolation performance at higher frequencies. MR dampers employed in the investigated structures enable us to change damping characteristics in real-time and require an external power supply on the signal level.

In terms of control action, semi-active systems are feedback systems. Their components are: sensors to detect vibrations, controller to manipulate the signals obtained from the sensors and MR damper(s) to influence the mechanical response of the structure. There are many approaches to control design of semi-active systems. Generally, they are based on control theory concepts. Controller configuration and parameters are dependent on the particular objectives to be satisfied as well as on the quantities which can be measured.

The schematic diagram of the investigated systems is shown in Figure 5. To measure structure motion we used displacement or acceleration sensors. The velocities were reproduced using derivative or integral blocks of Simulink. MR dampers were activated by a specially developed power controller using analog voltage signals (Sapiński 2006).

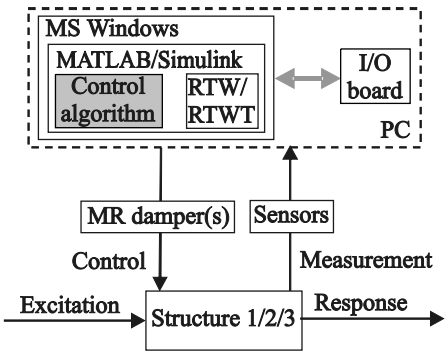

Fig. 5. Schematic diagram of the investigated systems

The applied measurement-control system comprises a PC with an I/O board installed and supported by MATLAB/Simulink and Real Time Workshop (RTW) toolbox, and extension Real Time Windows Target (RTWT) running on MS Windows. For control algorithm design we used MATLAB/Simulink which makes use of state-of-the-art tools for modeling and simulation, and has the required hardware for implementation of control algorithms. The RTW and RTWT extend the potential applications of MATLAB/Simulink for control, by providing an engineering path known as the rapid prototyping method (Fig. 6). This method enables the real-time implementation of controllers directly from Simulink.

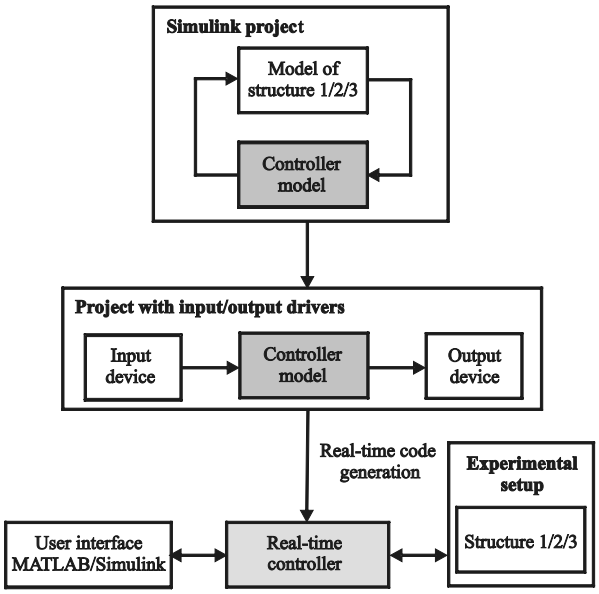

Fig. 6. Diagram of the rapid prototyping method

Since the RTW is not capable of generating real-time tasks in MS Windows, the environment is supported by RTWT. Communication procedures featured by RTWT allow the compilation of RTW code and its real-time operation in MS Windows on the specialist hardware platform. It should be noted that the generation of the real-time controller is fully automatic and no extra knowledge of real-time programming is necessary.

4. CONTROL OF AN MR DAMPER IN A DRIVER'S SEAT SUSPENSION

The structure 1 has one degree of freedom and is subjected to displacement excitations. The schematic diagram of the structure is shown in Figure 7 where: z – displacement of the shaker base, k – spring stiffness, c_r – damping coefficient of the MR damper corresponding to the current i operating in the coil, m – mass of the driver (sprung mass) and x – displacement of the driver. The control objective is to reduce vertical acceleration of the driver.

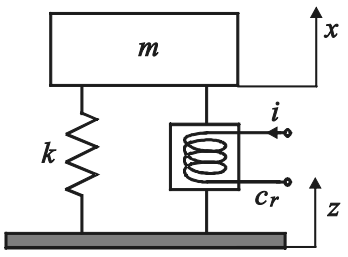

Fig. 7. Schematic diagram of structure 1

The parameters of the structure 1 are: mass of the driver m = 70 kg and stiffness coefficient of a bolt spring k = 26 300 N/m. The undamped natural frequency of structure is 3.1 Hz and the resonance frequency for no current in the damper is 4.1 Hz.

The photo of the system 1 ready for tests is shown in Figure 8.

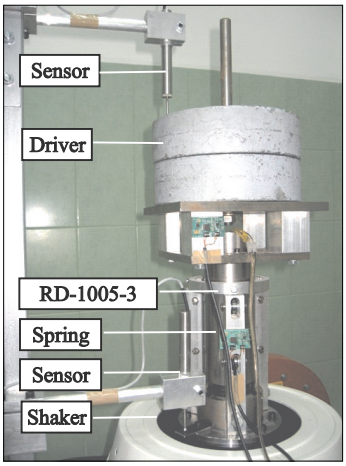

Fig. 8. System 1 ready for tests

In order to compare vibration isolation performance we introduce the vertical acceleration transmissibility factor:

$$T_{xz} = \frac{A_{\ddot{x}}}{A_{\ddot{z}}} \tag{1}$$

where $A_{\ddot{z}}$ is the amplitude of the shaker base acceleration and $A_{\ddot{x}}$ is the amplitude of the driver acceleration.

In the first stage we investigated the structure with a damper in the passive mode. The structure response was measured under sine displacement excitation with amplitude 3.8×10^{-3} m and frequency range (1, 10) Hz for current in the damper: 0.00, 0.10 and 0.20 A. The obtained acceleration transmissibility plots are provided in Figure 9. It appears that as the current in the damper increased, resonant frequency of the structure increased too.

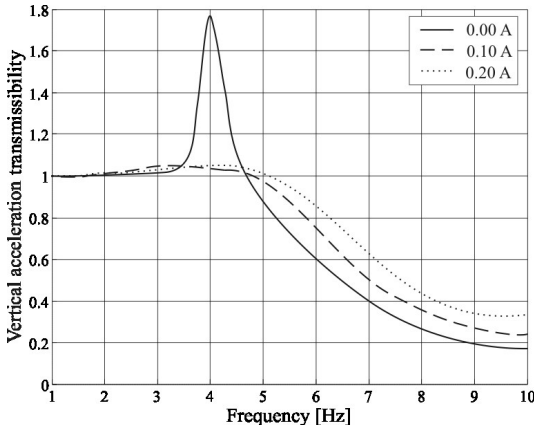

Fig. 9. Vertical acceleration transmissibility plots of system 1 with damper in the passive mode

In the second stage we investigated the structure with the damper in the active mode. To control the damper we applied: on-off algorithm (CS1) and fuzzy algorithm (CS2). The input signals for the algorithms are velocity of the

driver and relative velocity (the difference between velocity of the driver and the shaker base). The output signal was current in the damper switched in accordance with control laws.

The CS1 algorithm involves switching the current in the damper in between the maximal value and minimal value (no current) and the CS2 algorithm (with Mamdami inference system) switching the current in between five values (Sapiński 2006). The obtained vertical transmissibility plots (Fig. 10) reveal significant system performance improvement when compared with damper in the active mode with that with damper in the passive mode. The CS2 algorithm proves to be most effective as we gain best resonant frequency control and superior high frequency isolation.

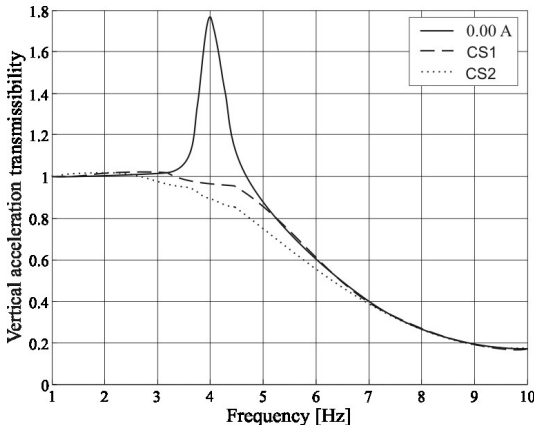

Fig. 10. Vertical acceleration transmissibility plots of system 1 with damper in the active mode

5. CONTROL OF MR DAMPERS IN A VEHICLE SUSPENSION

The structure 2 has two-degrees-of-freedom and is subjected to displacement excitations. The schematic diagram of the structure is shown in Figure 11. Such structure represents a pitch-plane model of a vehicle suspension an is considered applicable for study of off-road vehicle without tires or without primary suspensions.

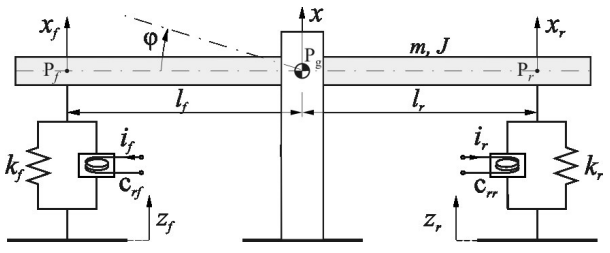

Fig. 11. Schematic diagram of structure 2

The structure comprises a stiff beam with the mass m and the moment of inertia J with respect to the beam's centre-of-gravity (cog) P_g, supported jointly at points P_f, P_r on identical spring-damper systems. The structure has two degrees of freedom: vertical displacement x and longitudinal bounce φ with regard to P_g. The mechanical constraints of the structure motion are ensured with rigid stabilizing vertical guides positioned symmetrically on two sides of the beam (to restrict the motion of the beam's cog). The beam is base-excited by the displacement z_f and z_r. The control objective is to minimize vertical and angular acceleration of the beam's cog.

The parameters of the structure 2 aredistance l_f = 0.7 m, distance l_r = 0.7 m, total length of the beam l = 1.5 m, m = 176.73 kg, J = 33.74 kg·m^2, stiffness coefficient k_f = = k_r = 42016 N/m.

The photo of the system ready for tests is shown in Figure 12.

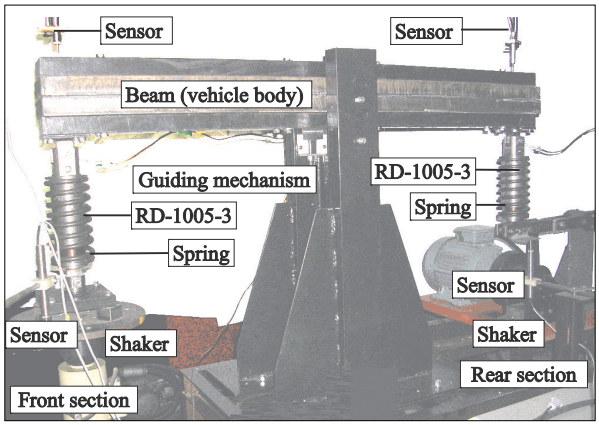

Fig. 12. System 2 ready for tests

In order to compare vibration isolation performance we introduce the *rms* vertical and angular transmissibility factors $T_{\ddot{x}}^{rms}$ and $T_{\ddot{\varphi}}^{rms}$ which are defined as follows (Martynowicz and Sapiński 2007):

$$T_{\ddot{x}}^{rms} = \frac{rms(\ddot{x})}{rms(\ddot{z}_x)} \tag{2}$$

where $rms(\ddot{x})$ is the *rms* value of the vertical acceleration of the beam c.o.g. and $rms(\ddot{z}_x)$ is the *rms* value of the mean vertical acceleration,

$$T_{\ddot{\varphi}}^{rms} = \frac{rms(\ddot{\varphi})}{rms(\ddot{z}_\varphi)} \tag{3}$$

where $rms(\ddot{\varphi})$ is the *rms* value of the angular acceleration of the beam with respect to its c.o.g. and $rms(\ddot{z}_\varphi)$ is the *rms* value of the mean angular acceleration.

To establish *rms* vertical acceleration transmissibility factor we applied sine excitations with the same frequency, amplitude and phase ($z_f = z_r$) to the suspension-set. Similarly to establish *rms* angular acceleration transmissibility factor we applied harmonic excitations with the same frequency, amplitude and opposite phase ($z_f = -z_r$).

In the first stage we investigated the structure with dampers in the passive mode. The structure response was measured under sine displacement excitation with amplitude 3.8×10^{-3} m and frequency range (2, 8) Hz for current in the damper: 0.00 and 0.25 A.

In the second stage we investigated the structure with dampers in the active mode by applying CV1 and CV2 algorithms to control the dampers. The CV1 algorithm is a semi-active embodiment of the skyhook control and indicates how to modulate the MR dampers that they emulate skyhook dampers (Martynowicz 2006). The CV2 algorithm (with Mamdami inference system) involves switching the current in the dampers in between thirteen values (Sapiński 2008).

The input signals for the CV1 and CV2 algorithms were velocities $\dot{x}_f$ and $\dot{x}_r$ and relative velocities $\dot{x}_f - \dot{z}_f$ and $\dot{x}_r - \dot{z}_r$. The output signals were currents in the dampers switched in accordance with control laws.

The obtained results shown in the form_of *rms* vertical acceleration transmissibility plots (Fig. 13) and angular acceleration transmissibility plots (Fig. 14) enable us to compare system performance for the dampers in the passive mode (current 0.00 and 0.25 A) with that in the active mode (algorithms CV1 and CV2).

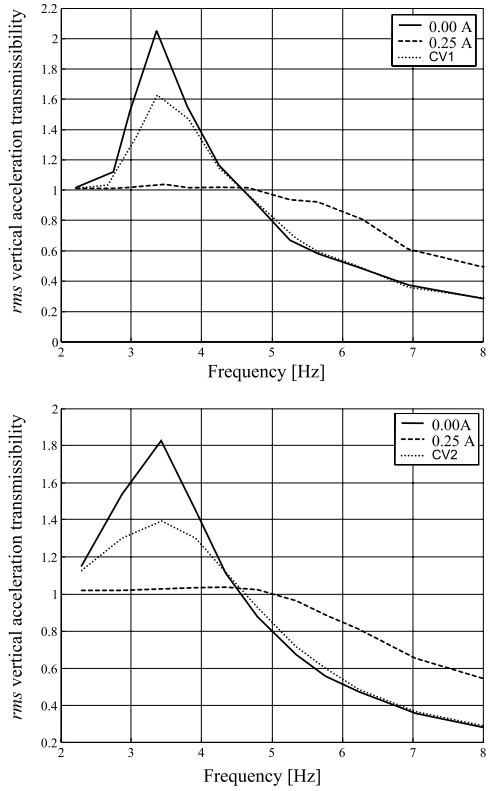

Fig. 13. Vertical acceleration transmissibility plots of system 2 with dampers in the passive and active mode

It is evident that resonance vibrations for the dampers in the active mode are reduced while compared to that in the passive mode for current 0.00 A. The CV2 algorithm exhibits better properties than the CV1 algorithm in the resonance range. It should be noted that super-resonance vibrations (mainly angular) increase for the CV2 algorithm when compared with the CV1 algorithm and current 0.00 A. The structure with dampers in the passive mode for 0.25 A exhibits the best properties within the range of (2.0, 4.5) Hz of vertical vibrations. Similarly within the range of (4.0, 6.7) Hz of angular vibrations. However, higher frequencies are poorly isolated.

6. CONTROL OF AN MR DAMPER ATTACHED TO A CABLE

The structure 3 has an infinite number of degrees of freedom and is manually excited. The schematic diagram of the structure is shown in Figure 14.

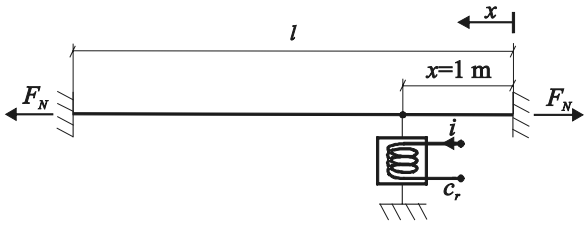

Fig. 14. Schematic diagram of structure 3

The structure comprises a horizontally suspended and stretched cable of the length l, linear density m_x and static tension force F_N, with an MR damper attached transversely to the cable at the distance x from the support. It is assumed that the damper acts upon the cable with a concentrated force related to the current in the damper. The control objective is to reduce transverse free vibrations of the cable.

An approximate formula to determine the optimal viscous damping coefficient c_{opt} of a viscous damper, attached at a small distance from the support x, is given by (Krenk 2000):

$$c_n^{(opt)} = \frac{1}{n\pi}\frac{1}{x}\sqrt{m_x F_N} \tag{4}$$

where n is the mode number.

The optimal value of the viscous damping coefficient for a cable with specified parameters and for the given damper location is different for each mode. A viscous damper optimally tuned to damp one mode of vibrations may not optimally damp other modes.

Capability of tuning of an MR damper to the occurring vibration mode proves to be its major advantage over conventional viscous dampers.

To control the damper the CC1 algorithm was applied which ensures that the damper should emulate a viscous damper with the desired value of viscous damping coefficient c_{des} (Fig. 15). It is assumed that the force generated by MR damper in active mode should be proportional to piston velocity (unlike in the passive mode when force depends on velocity in a minor degree only). For the given cable parameters, vibration modes and damper location, the coefficient c_{des} should be derived from Eq. (4) to ensure the maximal damping.

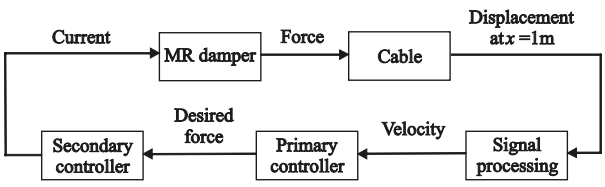

Fig. 15. Diagram of the CC1 algorithm

The CC1 algorithm utilizes the feedback loop from the piston velocity. This velocity in real conditions might be reconstructed from the acceleration or piston displacement signals. In the experiments the velocity signal was estimated on-line (Signal processing block) from the piston displacement. Knowing velocity, the desired force is obtained (Primary controller block) which is processed with the force tracking control system (Secondary controller block) to obtain current applied to the damper.

Ensuring satisfactory accuracy of the MR damper force tracking control is a major task in implementation of the control algorithm. Damping force control might be handled either by applying an internal feedback from the damper force, or with no force feedback, by applying an inverse model of the damper. In the study we applied the approach utilizing an inverse model of the MR damper (Maślanka *et al.* 2007, Maślanka 2008). Piston velocity and desired force are fed to the model input. The model output is current in the damper which should ensure the desired damping force.

The photo of the system ready for tests is shown in Figure 16.

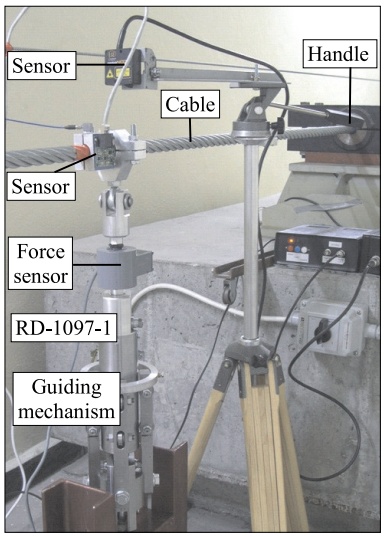

Fig. 16. System 3 ready for tests

Cable acceleration can be measured at maximally 12 points. Besides, there are laser sensors to measure cable displacements at two points. The damper force is measured along the damper axis.

As regards the CC1 algorithm, optimal values of viscous damping coefficient have to be estimated for the given parameters of the test facility and damper location. For the given cable parameters (l, m_x) the optimal viscous damping coefficient depends on the static tension force F_N, damper location x_d and the cable vibration mode. The tension force was taken to be 27 kN and the damper location x = 1 m, yielding c_{opt} value of about 2100 N·s/m for the first mode, 1050 N·s/m for the second mode and 700 N·s/m for the third one. The force range of the RD-1097-1 damper allows the optimal viscous damper force to be tracked only in a certain amplitude range for the given mode.

In the study we present results applied to the first mode of free vibration, excited manually at mid-point of the cable. The chief advantage of the free vibration test is that the basic analysis of recorded data yields relationships of damping and frequency as the function of amplitude.

In the first stage we investigated the cable with no damper. The measured quantity was displacement at the cable mid-point x = 15 m. Free vibration measurement data are compiled in Figure 17. The time when free vibrations begin is denoted as t_s.

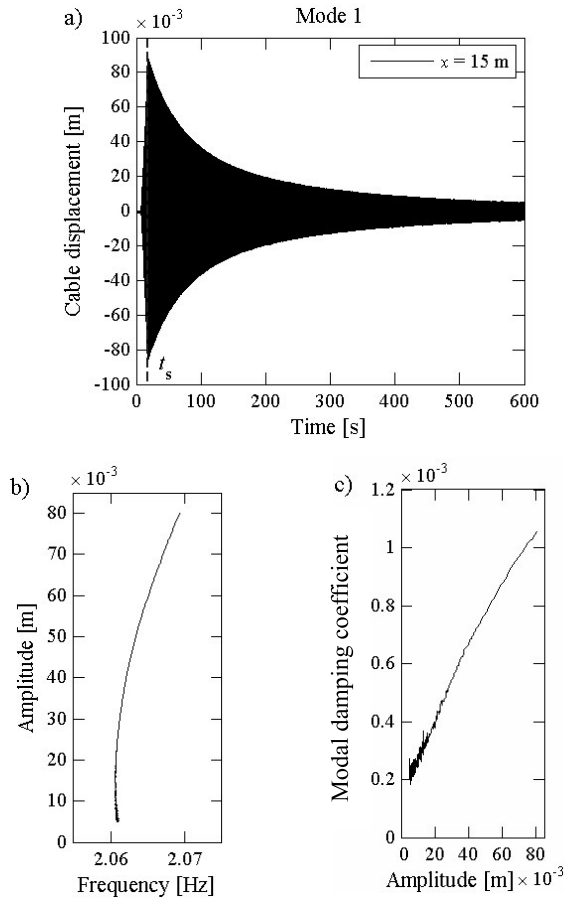

Fig. 17. System 3 with no damper: a) displacement decay at x = 15 m; b) amplitude vs. frequency; c) modal damping coefficient vs. amplitude

Cable vibration frequency and the modal damping coefficient are identified basing on the analysis of displacement envelope, yielding relationships between amplitude, frequency and modal damping coefficient (Figs. 17b and 17c). Dynamic component of the cable tension force increases with amplitude, which is revealed as a slight increase of free vibration frequency (Fig. 17b). The modal damping coefficient for the first mode varies from 0.2×10^{-3} for amplitude 5×10^{-3} m, to 1.05×10^{-3} for the amplitude 80×10^{-3} m. The obtained relationship between the modal damping coefficient and amplitude is approximately linear.

In the second stage we investigated the cable with the damper in the passive mode. Measured quantities include: cable displacement and acceleration at the damper location, cable displacement at mid-point and the force acting in the

damper axis. Of particular interest was the first mode of free vibrations. Current in the damper was set to be: 0.25 and 0.50 A. The obtained results are shown in Figures 18 and 19.

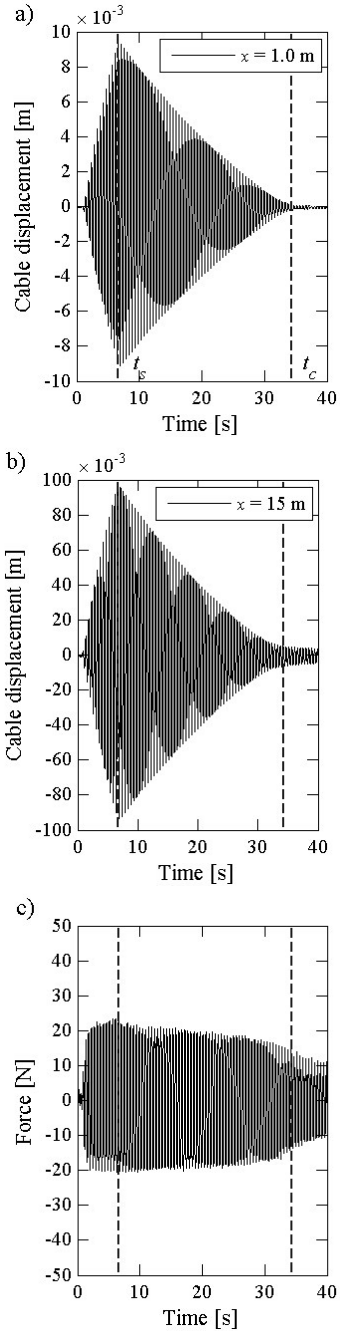

Fig. 18. System with damper in the passive mode; current 0.25 A: a) displacement at x = 1 m; b) displacement at x = 15 m; c) damper force

It is apparent that free vibration of the cable with the damper tends to decay much faster than that with no damper. One has to bear in mind, however, that the decay is accompanied by a minor variation of damper force amplitude (Figs. 18c and 19c). This very feature of the MR damper force leads to an adverse blocking effect of the damper piston movement.

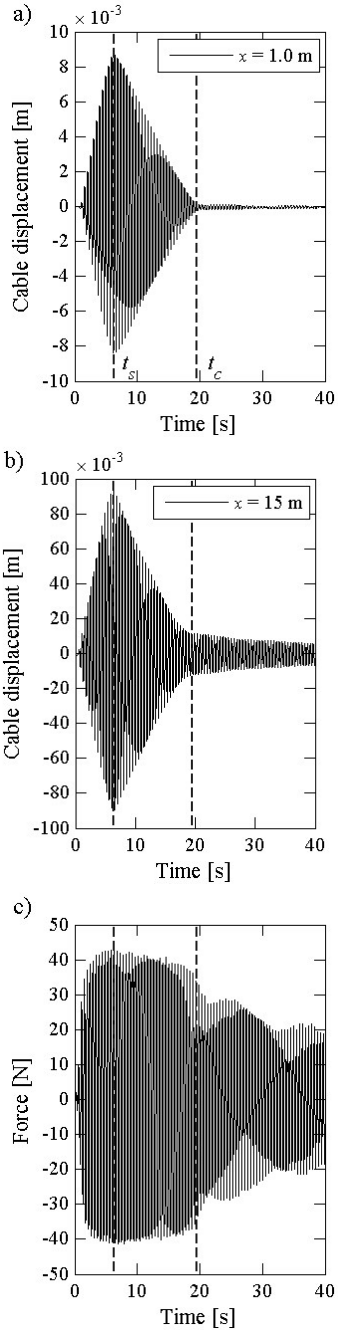

Fig. 19. System 3 with damper in the passive mode; current 0.50 A: a) displacement at x = 1 m; b) displacement at x = 15 m, c) damper force

Rapid decay of cable vibrations (the higher the current, the faster the vibration decay) is observed from the instant when free vibration begins right till the time when complete blocking of the damper occurs (denoted as t_c). The damper blocking is observed when an instantaneous force of cable action upon the damper is less than the force required to change the piston position, in the whole period of vibrations. As vibration amplitude decays, the force of cable action upon the damper is reduced whilst the current-dependent friction component of the damper restoring force remains unchanged. Comparison of these two forces allows for formulating the theoretical condition of MR damper

blocking (Weber *et al*. 2005). Plots of cable displacement at x = 1 m and at x = 15 m (Figs. 18a, 18b and 19a, 19b) indicate that when the damper stops working, the remaining part of the cable still vibrates with no appreciable damping. The point where x = 1 m becomes a node of a new, undamped mode with a slightly higher frequency

In the third stage we investigated the cable with damper in the active mode by applying CC1 algorithm. The obtained results for the first mode of free vibrations are shown in Figure 20.

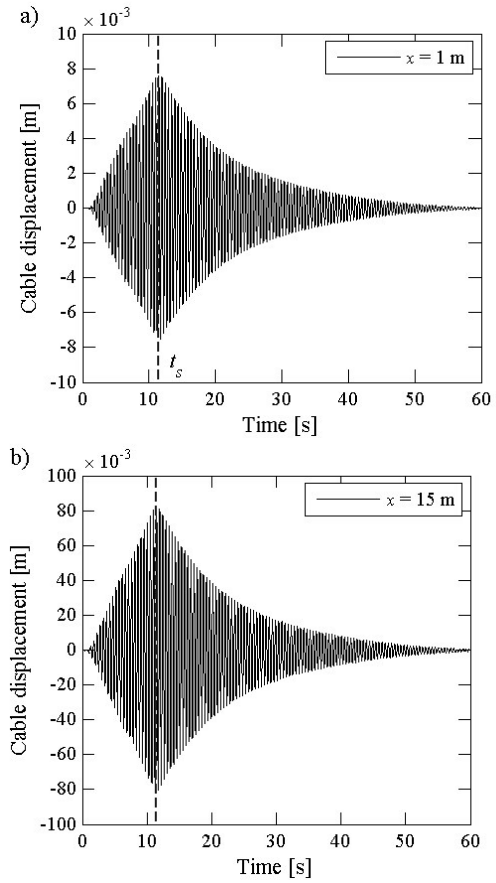

Fig. 20. System 3 with damper in the active mode; c_{des} = 500 Ns/m: a) displacement at x = 1 m; b) displacement at x = 15 m

Results were obtained for c_{des} = 500 N·s/m (this value of c_{des} = 500 Ns/m is equal to 25% of the optimal value for the first mode, due to the limited force generated by the RD-1097-1 damper).

The cable vibration decay plots for damper in the passive mode (Fig. 20) vastly differ from those for damper in the passive mode (Figs. 18 and 19). The vibration decay envelope has the shape similar to an exponential curve. Furthermore, displacement decay at x = 1 m (Fig. 20a) and at x = 15 m (Fig. 20b) proceeds in the same manner throughout the whole considered amplitude range. Application of the CC1 algorithm allows the damper blocking effect to be almost entirely eliminated. The system comprising a cable with damper in active mode displays the properties of a viscous-damped system.

7. SUMMARY

MR dampers acting as interfaces between the electronic control systems and mechanical structures demonstrate the effectiveness for providing real-time vibration control. They prove to be a good choice for applications where strong dynamic feature is required.

MR damper-based vibration control systems exhibit several advantages such as: mechanical simplicity, continuous change of damping characteristics, high dynamic range, fast and noiseless work, robustness, and low power demands.

The study illustrates potentials of MR dampers in vibration control at the example of three mechanical structures which were investigated experimentally. The obtained results demonstrate significant system performance improvement achieved through the control of MR damper(s).

References

Krenk S. 2000, *Vibrations of a taut cable with an external damper*. Journal of Applied Mechanics, vol. 67, 772–776.

Martynowicz P. 2006, *Synteza algorytmów sterowania drganiami dla płaskiego modelu magnetoreologicznego zawieszenia pojazdu* (in Polish). Doctoral Dissertation, AGH University of Science and Technology.

Martynowicz P., Sapiński B. 2007, *Experimental study of vibration control in a 2 DOF pitch-plane model of a magnetorheological vehicle suspension*. Quarterly Mechanics, vol. 26, No. 2, 772–776.

Maślanka M., Sapiński B., Snamina J. 2007, *Experimental study of vibration control with an attached MR damper*. Journal of Theoretical and Applied Mechanics, vol. 45, No. 4, 874–893.

Maślanka M. 2008, *Semiaktywny układ redukcji drgań liny z tłumikiem magnetoreologicznym* (in Polish). Doctoral Dissertation, AGH University of Science and Technology.

Sapiński B. 2006, *Magnetorheological Dampers in Vibration Control*. AGH University of Science and Technology Press, Cracow, Poland.

Sapiński B. 2008, *Real-time Control of Magnetorheological Dampers in Mechanical Systems*. AGH University of Science and Technology Press, Cracow, Poland.

Weber F., Feltrin G., Motavalli M. 2005, *Passive damping of cables with MR dampers*. Materials and Structures, vol. 38, 568–577.